

# PlanarSplatting: Accurate Planar Surface Reconstruction in 3 Minutes

## Supplementary Material

Our supplementary material contains two parts: 1) a PDF file that illustrates more details and results of our *PlanarSplatting*; and 2) a video file that shows the optimization process of our *PlanarSplatting*. Please refer to ‘*PlanarSplatting\_video.mp4*’ for more details.

### A. More Details of *PlanarSplatting*

#### A.1. Data Preparation for Optimization

On both the ScanNetV2 [1] and ScanNet++ [8] datasets, we used images sized at  $480 \times 640$  for our *PlanarSplatting*. On the ScanNetV2 dataset, we sample images for optimization from the original video at intervals of 8 frames. On the ScanNet++ dataset, we sample images for optimization from the original video at intervals of 10 frames.

#### A.2. Explanation of Eqs.(7)-(9)

As shown in Fig. S1, if  $|\mathcal{P}_X| \leq r_\pi^{x+}$ , we have  $2\sigma(5\lambda(r_\pi^{x+} - |\mathcal{P}_X|)) \geq 1.0$ . **Note that in practice, we clamp the maximum value of  $2\sigma(\cdot)$  to 1.** Then, together with Eqs.(7)-(9) in the main paper, the splatting weight of intersection point  $\mathbf{x}_\pi^r$  equals to 1 if it is located within the physical region of plane primitive. The splatting weight attenuates when the point falls outside the plane primitive.

#### A.3. Optimization Details

The learning rates of the learnable plane centers, plane radii, and plane rotation are all fixed at 0.001. We introduce Plane Splitting during optimization to better fit the scene geometry. In Fig. S2, we present two examples to explain our Plane Splitting operation along the X-axis and Y-axis of the 3D plane primitive.

### B. More Ablations

#### B.1. Ablation of Plane Splitting

In Tab. S1, we show the results of using different splitting thresholds during optimization and find that 0.2 works well to balance all metrics.

#### B.2. Ablation of Depth and Normal Supervision

We also evaluate the influence of depth and normal supervision. For depth supervision, we use two types of depth in ablation studies, including Metric3Dv2 [3] depth and sensor depth. For normal supervision, we utilize two types of normals in ablation studies, namely Omnidata [2] normal and Metric3Dv2 [3] normal. As shown in Tab. S2, using both the depth and normal supervisions improves the

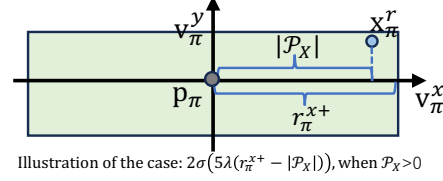


Figure S1. Explanation of the planar splatting function.

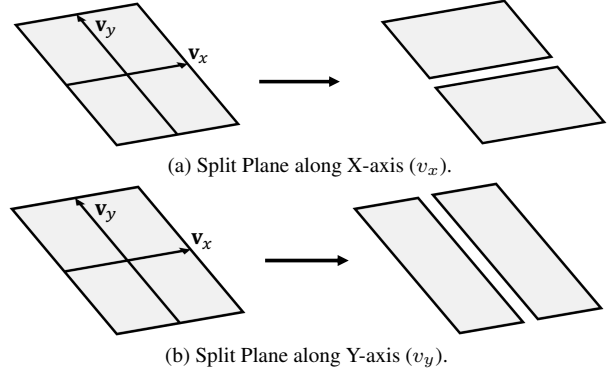


Figure S2. Illustration of Plane Splitting.

Table S1. Ablation of plane splitting threshold. ‘#Prim.’: number of 3D planar primitives.

Threshold	Geometry		Segmentation			Planar	#
	Chamfer ↓	F-score ↑	VOI ↓	RI ↑	SC ↑	Chamfer ↓	
0.1	<b>4.66</b>	71.25	2.487	0.958	0.536	<b>9.09</b>	2069
0.2	<b>4.66</b>	<b>71.30</b>	<u>2.473</u>	<u>0.958</u>	<b>0.541</b>	<u>9.25</u>	1669
0.3	<u>4.68</u>	71.24	<b>2.471</b>	<b>0.959</b>	<u>0.539</u>	9.43	1573

modeling of plane shape and further enhances all metrics compared with the depth-only results.

#### B.3. Ablation of NVS

We evaluate the effectiveness of our planar reconstruction for novel view synthesis (NVS) by comparing with it different initializations. As shown in Tab. S3, the better rendering quality are benefited from the better initialization by our geometries, and the well-initialized point positions can be fixed during the optimization of 2D/3D-GS [4, 5].

### C. More Qualitative Results

#### C.1. Novel View Synthesis

In Fig. S3, we show more novel view synthesis results on the ScanNetV2 [1] dataset. By combining our *PlanarSplatting* with 2DGS [4] and 3DGS [5], the rendering results are

Table S2. Ablation of depth and normal supervision.

Settings		Geometry	Segmentation	Planar	Settings		Geometry	Segmentation	Planar
Depth	Normal	Chamfer ↓	VOI ↓	Chamfer ↓	Depth	Normal	Chamfer ↓	VOI ↓	Chamfer ↓
Metric3Dv2	Metric3Dv2	<b>4.08</b>	<b>2.272</b>	<b>9.10</b>	Sensor	Metric3Dv2	<b>3.69</b>	<b>2.259</b>	<b>8.80</b>
Metric3Dv2	-	4.41	2.648	10.81	Sensor	-	3.86	2.410	9.87

Table S3. NVS Ablation. ‘P.P.’: Point Position. ‘Mv2’: Metric3Dv2.

Fix P.P.	Init.		PSNR ↑	SSIM ↑	LPIPS ↓		PSNR ↑	SSIM ↑	LPIPS ↓
No	SfM	3DGS	24.417	0.781	0.321	2DGS	24.766	0.796	0.323
Yes	Mv2	3DGS	25.265	0.813	0.308	2DGS	25.170	0.811	0.309
No	Ours	3DGS	25.225	0.811	<b>0.292</b>	2DGS	25.142	0.809	<b>0.293</b>
Yes	Ours	3DGS	<b>25.471</b>	<b>0.816</b>	0.296	2DGS	<b>25.380</b>	<b>0.813</b>	0.296

significantly improved.

## C.2. Planar Reconstruction

In Fig. S4, Fig. S5, and Fig. S6, we show more planar reconstruction results on the ScanNetV2 [1] and ScanNet++ [8] datasets. Compared to the baselines including 2DGS [4]+RANSAC, PlanarRecon [7] and AirPlanes [6], our *PlanarSplatting* can achieve more accurate and complete plane reconstruction results, demonstrating the superiority of our proposed *PlanarSplatting*.

## References

- [1] Angela Dai, Angel X. Chang, Manolis Savva, Maciej Halber, Thomas A. Funkhouser, and Matthias Nießner. Scannet: Richly-annotated 3d reconstructions of indoor scenes. In *IEEE Conf. Comput. Vis. Pattern Recog.*, pages 2432–2443, 2017. **1, 2, 3, 4**
- [2] Ainaz Eftekhari, Alexander Sax, Jitendra Malik, and Amir Zamir. Omnidata: A scalable pipeline for making multi-task mid-level vision datasets from 3d scans. In *Int. Conf. Comput. Vis.*, pages 10766–10776, 2021. **1**
- [3] Mu Hu, Wei Yin, Chi Zhang, Zhipeng Cai, Xiaoxiao Long, Hao Chen, Kaixuan Wang, Gang Yu, Chunhua Shen, and Shaojie Shen. Metric3d v2: A versatile monocular geometric foundation model for zero-shot metric depth and surface normal estimation. *IEEE Trans. Pattern Anal. Mach. Intell.*, 46(12):10579–10596, 2024. **1**
- [4] Binbin Huang, Zehao Yu, Anpei Chen, Andreas Geiger, and Shenghua Gao. 2d gaussian splatting for geometrically accurate radiance fields. In *ACM SIGGRAPH Conference Papers*, page 32, 2024. **1, 2**
- [5] Bernhard Kerbl, Georgios Kopanas, Thomas Leimkühler, and George Drettakis. 3d gaussian splatting for real-time radiance field rendering. *ACM Trans. Graph.*, 42(4):139:1–139:14, 2023. **1**
- [6] Jamie Watson, Filippo Aleotti, Mohamed Sayed, Zawar Qureshi, Oisín Mac Aodha, Gabriel J. Brostow, Michael Firman, and Sara Vicente. Airplanes: Accurate plane estimation

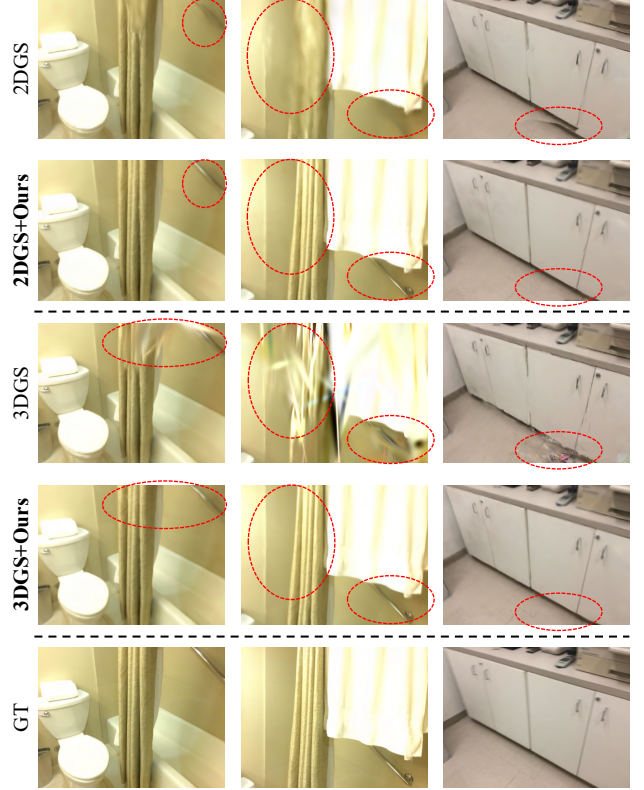


Figure S3. More qualitative comparisons of novel view synthesis on the ScanNetV2 [1] dataset.

- via 3d-consistent embeddings. In *IEEE Conf. Comput. Vis. Pattern Recog.*, pages 5270–5280, 2024. **2**
- [7] Yiming Xie, Matheus Gadelha, Fengting Yang, Xiaowei Zhou, and Huaizu Jiang. Planarrecon: Realtime 3d plane detection and reconstruction from posed monocular videos. In *IEEE Conf. Comput. Vis. Pattern Recog.*, pages 6209–6218, 2022. **2**
- [8] Chandan Yeshwanth, Yueh-Cheng Liu, Matthias Nießner, and Angela Dai. Scannet++: A high-fidelity dataset of 3d indoor scenes. In *Int. Conf. Comput. Vis.*, pages 12–22, 2023. **1, 2, 5**

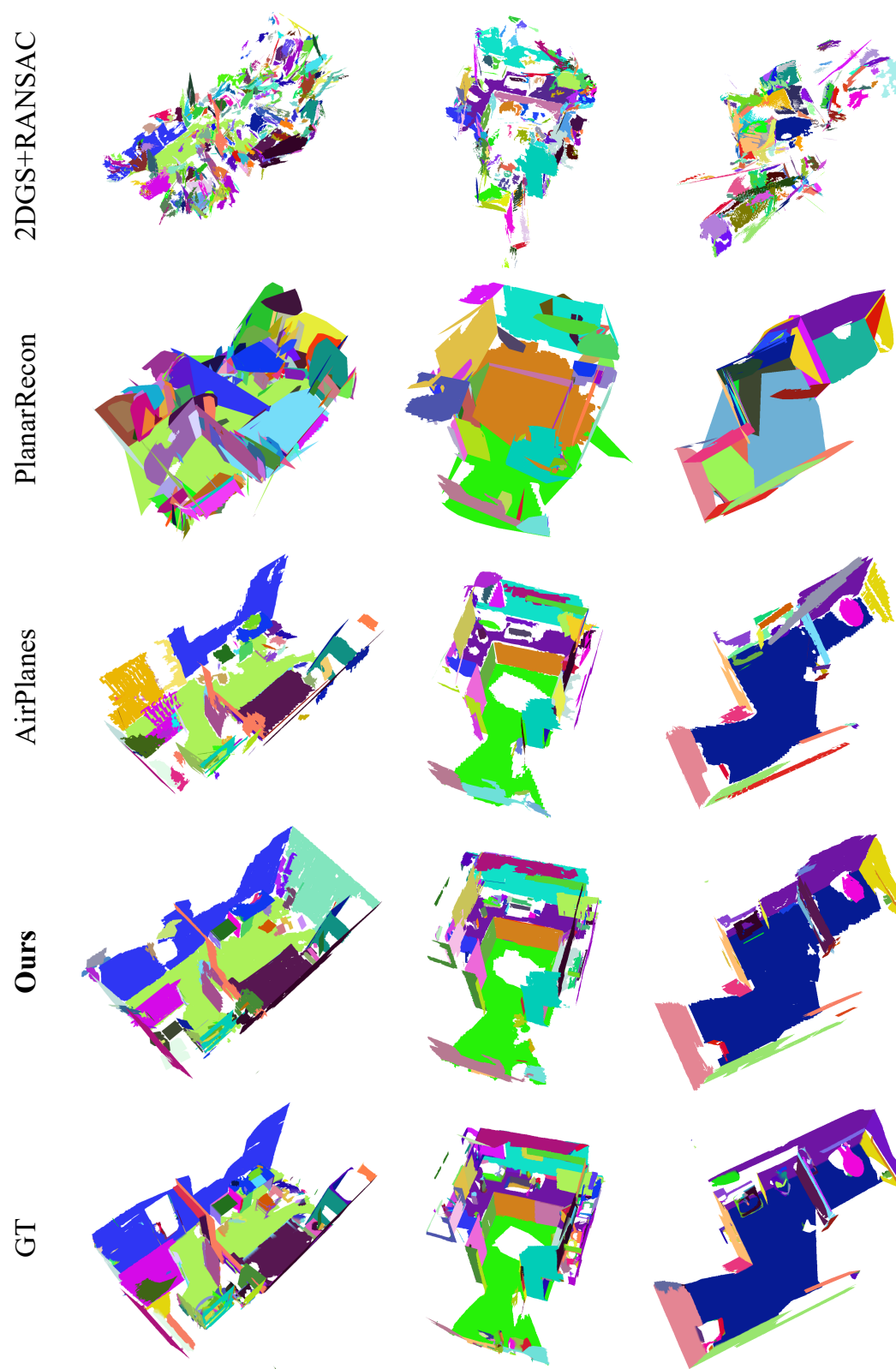


Figure S4. More qualitative comparisons of planar reconstruction on the ScanNetV2 [1] dataset.

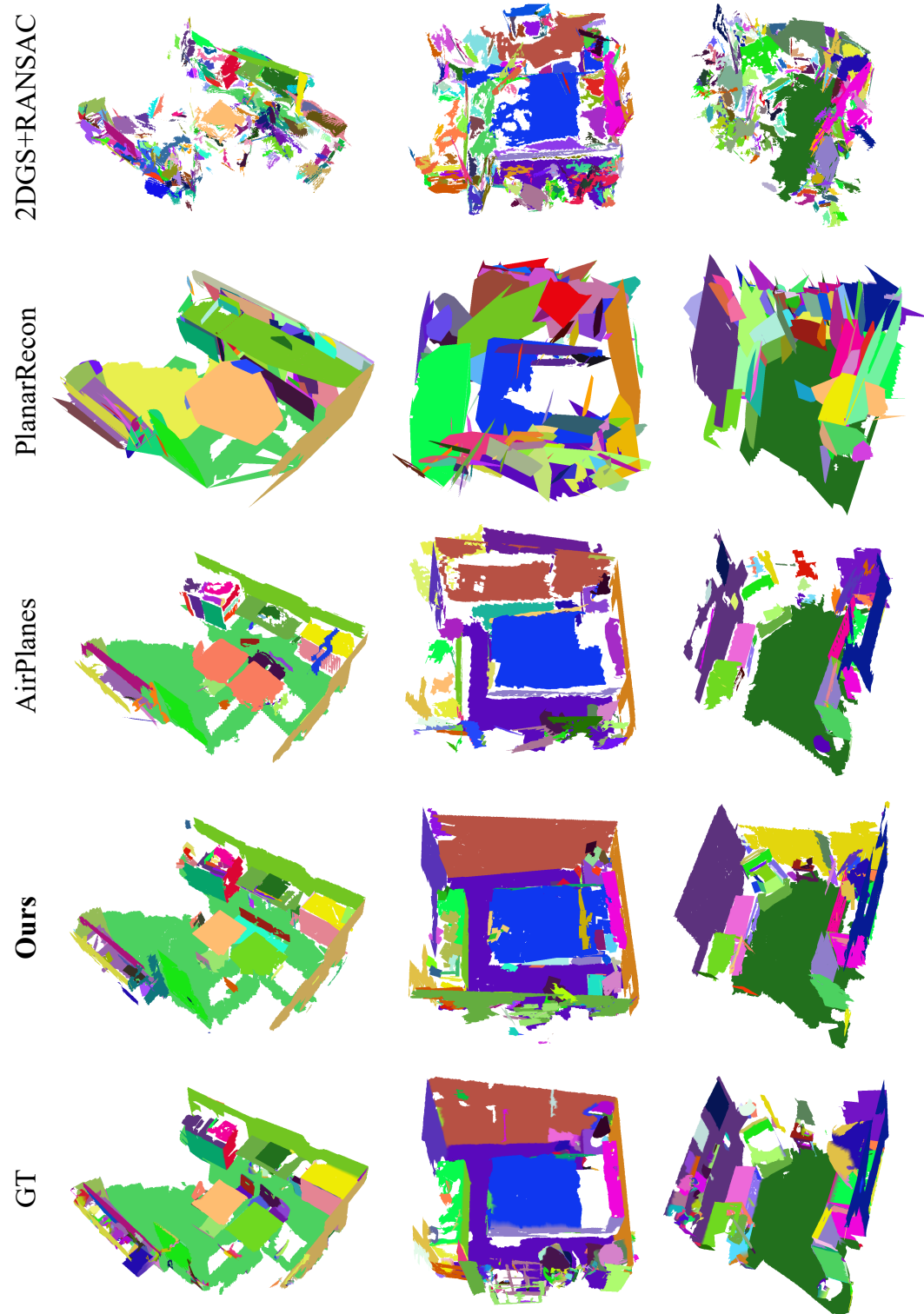


Figure S5. More qualitative comparisons of planar reconstruction on the ScanNetV2 [1] dataset.

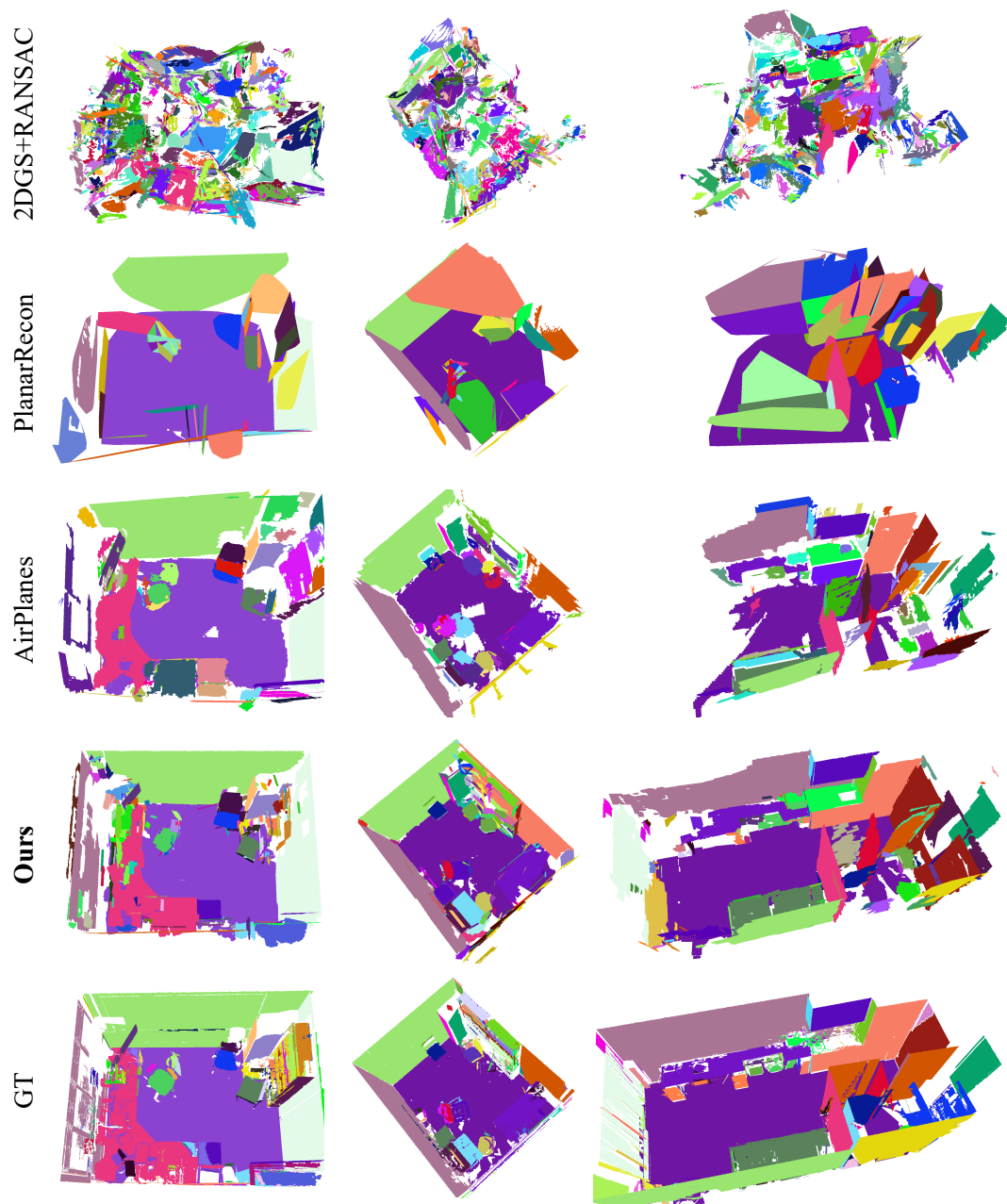


Figure S6. More qualitative comparisons of planar reconstruction on the ScanNet++ [8] dataset.